Chapter 2

Diffusion Theory

2.1 Chapter Summary

The evolution of ice in diffusive contact with a planet's atmosphere through a barrier of porous material is affected by the thermal and geometric properties of the regolith. The former controls the propagation of diurnal, annual, and long-term thermal waves into the subsurface and thereby modulates the temperatures experienced at depth. The latter set of properties, including porosity, pore size and shape, and tortuosity, influence the rate at which gas molecules migrate in response to chemical potential gradients. Temperature, through its effect on the saturation vapor density of air and the vapor pressure of ice, determines the concentration of water molecules in the subsurface. Changing temperatures may create a positive, negative, or identically zero concentration gradient with respect to the vapor density in the atmosphere. If a gradient of concentration exists, there will be a net flux of water molecules down the gradient, resulting in a net growth or depletion of the subsurface ice with time, even under isobaric conditions. The magnitude of this flux depends both on the magnitude of the concentration gradient and on the diffusive properties of the soil, as represented by the diffusion coefficient, D.

Here expressions are developed for vapor transport in a sublimation environment where temperature and pressure can change with time and space. Gas-kinetic models for determining diffusion coefficients are presented, as well as some summarized empirical observations. The distinction between two primary types of diffusion, Fickian and Knudsen, are described, as are methods for handling the transition between the two regimes. Tortuosity is discussed and several methods for extracting this dimensionless geometric property of a porous medium are presented. Effects other than concentration diffusion that may operate in experimental apparatus as well as in natural environments are examined. Finally, the governing equation for ice deposition via diffusion is given.

Throughout this work, subscript 1 refers to H_2O and subscript 2 to the carrier gas, usually CO_2. For example, p_1 is the partial pressure of H_2O and ρ_1 the density of water vapor. The total pressure is denoted by $p_0 = p_1 + p_2$ and the total mass density by $\rho_0 = \rho_1 + \rho_2$. A script $\mathcal{D}$ refers to free-gas

diffusion coefficients while roman italic D refers to diffusion in a porous medium.

2.2 Vapor Transport

Diffusion of mass is due to differences in concentration, temperature, and pressure (*Reid et al.*, 1987). The general expression for diffusive flux of one dilute gas (species 1) in another (species 2) at low velocities is (*Landau and Lifshitz*, 1987, §57, §58)

$$J_{\text{Diff}} = -\rho_0 \left[\mathcal{D}_{12} \frac{\partial}{\partial z} \frac{\rho_1}{\rho_0} + \frac{\mathcal{D}_T}{T} \frac{\partial T}{\partial z} + \frac{\mathcal{D}_p}{p_0} \frac{\partial p_0}{\partial z} \right], \tag{2.1}$$

where J_{Diff} is the diffusive mass flux of gas 1, $\mathcal{D}_{12}$ the mutual diffusion coefficient, $\mathcal{D}_T$ the coefficient for "thermodiffusion", T the temperature, and $\mathcal{D}_p$ the coefficient of "barodiffusion". Thermodiffusion and barodiffusion are usually small compared with concentration diffusion (see sections 2.6.2 and 2.6.3).

Equation (2.1) holds in a reference frame where the center of mass velocity of the gas mixture is zero. In an environment where temperature and total pressure change little, and the vapor concentration is low, the concentration diffusion J_{Diff} would be simply described by

$$J_{\text{Diff}} = -\mathcal{D}_{12} \frac{\partial \rho_1}{\partial z}. \tag{2.2}$$

For a detailed discussion of reference frames and non-isothermal diffusion laws, see *Cunningham and Williams* (1980).

The porosity, ϕ, of a porous medium restricts the cross-sectional area available for transport. A second factor called tortuosity, τ, accounts for the increase in path length which the molecules must follow. The diffusion coefficient in a porous medium in the Fickian diffusion regime, D_{F}, can be written as (*Mason and Malinauskas*, 1983)

$$D_{\text{F}} = \frac{\phi}{\tau} \mathcal{D}_{12}. \tag{2.3}$$

The ratio ϕ/τ is also called the "obstruction factor". In principle, this reduction in diffusivity can be obtained theoretically from the void space geometry. In practice, the void space geometry is seldom known, even for soils in a laboratory environment.

In a porous medium, equation (2.2) is replaced by

$$J_{\text{Diff}} = -D \frac{\partial \rho_1}{\partial z}, \tag{2.4}$$

where J_{Diff} is the flux due to concentration diffusion. The effective diffusion coefficient, D, subsumes all effects of gas molecule collisions with pore walls and other gas molecules, and the geometry of

the pore spaces through which gas travels.

2.3 Diffusion Coefficient

The coefficient of diffusion is the product of mean velocity and mean free path, with a prefactor that can be temperature dependent. The mean velocity depends only on temperature; the mean free path is inversely proportional to the density of the gas. Thus, a thinner atmosphere has a higher diffusivity. The diffusivity of an unconfined gas at rest, in which molecules diffuse through an interstitial gas, forms the basis for understanding the diffusivity of a porous regolith.

Theoretical expressions can be obtained for the diffusion coefficient, $\mathcal{D}_{12}$, in a dilute gas at rest consisting of vapor species 1 and 2. The coefficient of self-diffusion, $\mathcal{D}_{11}$, is not measured in these experiments.

The coefficient of diffusion in a binary mixture of rigid elastic spherical molecules is, to first order in the density of the diffusing species, (*Chapman and Cowling*, 1970)

$$\mathcal{D}_{12} = \frac{3}{8 n_0 \sigma_{12}^2} \sqrt{\frac{k_B T}{2\pi} \left(\frac{1}{m_1} + \frac{1}{m_2} \right)}. \tag{2.5}$$

The number density n_0 is obtained from the ideal gas law, $n_0 = p_0/k_B T$, $\pi\sigma_{12}^2$ is the scattering cross section, k_B is the Boltzmann constant, and m_1 and m_2 are the molecular masses.

The parameter σ_{12} is computed by averaging the molecular radii of each species, $\sigma_{12} = (\sigma_1 + \sigma_2)/2$. The cross section for individual molecules can be determined from viscosity measurements of pure gases. *Chapman and Cowling* (1970) report molecular radii for CO_2 and N_2. *Schwertz and Brow* (1951) calculate a molecular radius for H_2O from the molecular volume of the liquid. The values are listed in Table 2.1.

For intermolecular forces other than a model of rigid elastic spheres, a temperature-dependent prefactor is introduced via the collision integral $\Omega_{12}(T)$ (*Mason and Malinauskas*, 1983; *Reid et al.*,

Parameter	Value	Reference
σ^{hes} (CO_2, N_2)	4.63, 3.76 Å	*Chapman and Cowling* (1970)
σ^{hes} (H_2O)	2.7 Å	*Schwertz and Brow* (1951)
σ^{LJ} (H_2O, CO_2, N_2)	2.641, 3.941, 3.798 Å	*Reid et al.* (1987)
ϵ/k (H_2O, CO_2, N_2)	809.1, 195.2, 71.4 K	*Reid et al.* (1987)

Table 2.1: Model parameters for the mutual diffusion coefficient. σ^{hes} = molecular radius of hard elastic spheres, σ^{LJ} and ϵ/k are parameters of the Lennard-Jones potential. The collision integral for the Lennard-Jones potential can be expressed as $\Omega_{12} = A(T^*)^{-B} + Ce^{-DT^*} + Ee^{-FT^*} + Ge^{-HT^*}$. Values for the constants A, B, C, D, E, F, G, H are given in *Neufeld et al.* (1972) and *Reid et al.* (1987). The dimensionless temperature T^* is given by $T^* = k_B T/\epsilon_{12}$ and the molecule specific parameter ϵ is computed for a gas pair by $\epsilon_{12} = \sqrt{\epsilon_1 \epsilon_2}$.

1987),

$$\mathcal{D}_{12} = \frac{3}{8 n_0 \sigma_{12}^2} \sqrt{\frac{k_B T}{2\pi} \left(\frac{1}{m_1} + \frac{1}{m_2} \right)} \frac{1}{\Omega_{12}(T)}. \tag{2.6}$$

The length parameter σ_{12} now depends on the intermolecular force law and its value is not the same as for the rigid elastic spherical molecules. For a Lennard-Jones potential, the function $\Omega_{12}(T)$ and parameters for H_2O, CO_2, and N_2 are given in Table 2.1.

For an ideal gas of hard elastic spheres, the diffusion coefficient depends on temperature as $T^{3/2}$, as can be seen from equation (2.5). For other intermolecular potentials, the temperature dependence is described by equation (2.6), and can be shown to have an exponent between 0 and 2. The free-gas diffusion coefficient is inversely proportional to pressure for any intermolecular potential.

Equation (2.6) is a first-order expansion derived from Chapman-Enskog theory. To lowest order, the diffusion coefficient does not depend on the relative concentration of the two gases, n_1/n_2, but only on the total number density, $n_0 = n_1 + n_2$, and on the temperature. Hence the diffusion coefficient is symmetric, $\mathcal{D}_{12} = \mathcal{D}_{21}$.

The second-order approximation of the diffusion coefficient introduces a dependence on n_1/n_2 (*Chapman and Cowling*, 1970). For a hard sphere model and low concentrations of species 1 ($n_1 \ll n_2$), the diffusion coefficient is increased by a factor of

$$\frac{1}{1 - m_1^2/(13m_1^2 + 30m_2^2 + 16m_1 m_2)}.$$

For low H_2O concentration in a CO_2 or N_2 atmosphere, this correction is <1%. The maximum correction for any mixing ratio for H_2O–CO_2 is 4%, and for H_2O–N_2 it is 2%, both occurring as $n_2 \to 0$. Hence the dependence of the diffusion coefficient on the proportions of the mixture can be neglected in comparison to other uncertainties.

Holman (1997) gives a semiempirical equation by *Gilliland et al.* (1974)

$$\mathcal{D}_{12} = 435.7 \mathrm{cm^2 s^{-1}} \frac{T^{3/2}}{p_0 (V_1^{1/3} + V_2^{1/3})^2} \sqrt{\frac{1}{M_1} + \frac{1}{M_2}},$$

where T is in Kelvin, p is in pascals, V_1 and V_2 are molecular volumes of gases 1 and 2, and M_1 and M_2 are their molar weights. Holman cautions that this expression is useful for various mixtures, but should not be used in place of experimental values of $\mathcal{D}_{12}$ when available.

The coefficient of mutual diffusion $\mathcal{D}_{12}$ has been directly measured from evaporation rates of water into pure gases. Measurements for H_2O–CO_2 are reported or compiled by *Guglielmo* (1882), *Winkelmann* (1884a,b, 1889), *Trautz and Müller* (1935a,b), *Schwertz and Brow* (1951), *Rossie* (1953), and *Crider* (1956) in the temperature range 291–373 K at atmospheric pressure. *Nagata and Hasegawa* (1970) use gas chromatography to determine the diffusivity at 394 K and higher temperatures. The International Critical Tables (*Washburn et al.*, 2003) list $\mathcal{D}_{\mathrm{H_2O \cdot CO_2}} =$

$(0.1387\ \mathrm{cm^2 s^{-1}})(T/T_0)^2(p_{\mathrm{ref}}/p)$, citing experiments by Guglielmo and Winkelmann. A comprehensive review of gaseous diffusion coefficients by *Marrero and Mason* (1972) recommends $\mathcal{D}_{\mathrm{H_2O\cdot CO_2}} = (9.24\times10^{-5}\ \mathrm{cm^2 s^{-1}})T^{3/2}\exp(-307.9/T)(p_{\mathrm{ref}}/p)$ for T in the range 296–1640 K. A diffusivity scaling often cited in the context of Mars studies is from *Wallace and Sagan* (1979), who use a prefactor determined from *Schwertz and Brow* (1951) to write $\mathcal{D}_{\mathrm{H_2O\cdot CO_2}} = (0.1654\mathrm{cm^2 s^{-1}})(T/T_0)^{3/2}(p_{\mathrm{ref}}/p_0)$. In all cases, $p_{\mathrm{ref}} = 1013$ mbar and $T_0 = 273.15$ K.

Measurements for H_2O–N_2 are available from *Hippenmeyer* (1949), *Schwertz and Brow* (1951), *Bose and Chakraborty* (1955–56), *Crider* (1956), *Nelson* (1956), and *O'Connell et al.* (1969) in the range 273–373 K. *Marrero and Mason* (1972) recommend $\mathcal{D}_{\mathrm{H_2O\cdot N_2}} = (1.87\times10^{-6}\ \mathrm{cm^2 s^{-1}})\times T^{2.072}(p_{\mathrm{ref}}/p_0)$ in the temperature range 282–373 K.

Figure 2.1 shows theoretical and experimental values of the mutual diffusion coefficient as a function of temperature. The empirical fits from *Marrero and Mason* (1972) and the International Critical Tables are based on measurements at high temperature and may not provide accurate results when extrapolated below 273 K. The empirical fits, the theoretical formula for a Lennard-Jones potential, and the theoretical formula for hard elastic spherical molecules predict slightly different temperature dependences. Measurement errors and uncertainties in cross sections introduce additional deviations that limit the accuracy to which diffusion coefficients can be computed for a free gas.

The Martian atmosphere consists of 95% CO_2, the next most abundant gases being nitrogen and argon. The fraction of gases other than CO_2 is small enough to be ignored and we consider a pure CO_2 atmosphere. According to the elastic hard sphere model, equation (2.5), the diffusion coefficient in CO_2 is smaller than in N_2 at the same pressure and temperature by a factor of

$$\frac{\mathcal{D}_{\mathrm{H_2O\cdot CO_2}}}{\mathcal{D}_{\mathrm{H_2O\cdot N_2}}} = \frac{\sigma^2_{\mathrm{H_2O\cdot N_2}}}{\sigma^2_{\mathrm{H_2O\cdot CO_2}}}\frac{\sqrt{1/18+1/44}}{\sqrt{1/18+1/28}} \approx 0.72. \tag{2.7}$$

Assuming a Lennard-Jones potential, this ratio would be 0.68–0.69 in the temperature range 150–293 K.

2.4 Mean Free Path and Knudsen Diffusion

The mean free path for species 1, diffusing in a gas composed of species 1 and 2, is (*Chapman and Cowling*, 1970)

$$\lambda_1 = \frac{1}{n_1\pi\sigma_{11}^2\sqrt{2} + n_2\pi\sigma_{12}^2\sqrt{1+m_1/m_2}}. \tag{2.8}$$

When only one gas is present, the familiar formula $\lambda_1 = 1/(\sqrt{2}n\pi\sigma^2)$ is recovered. When $n_1 \ll n_2$, the first term in the denominator, resulting from like-molecule collisions, is negligible. With this expression, the mean free path of H_2O in a dry CO_2 atmosphere at 600 Pa and 200 K is $\lambda_1 \approx 9$ μm.

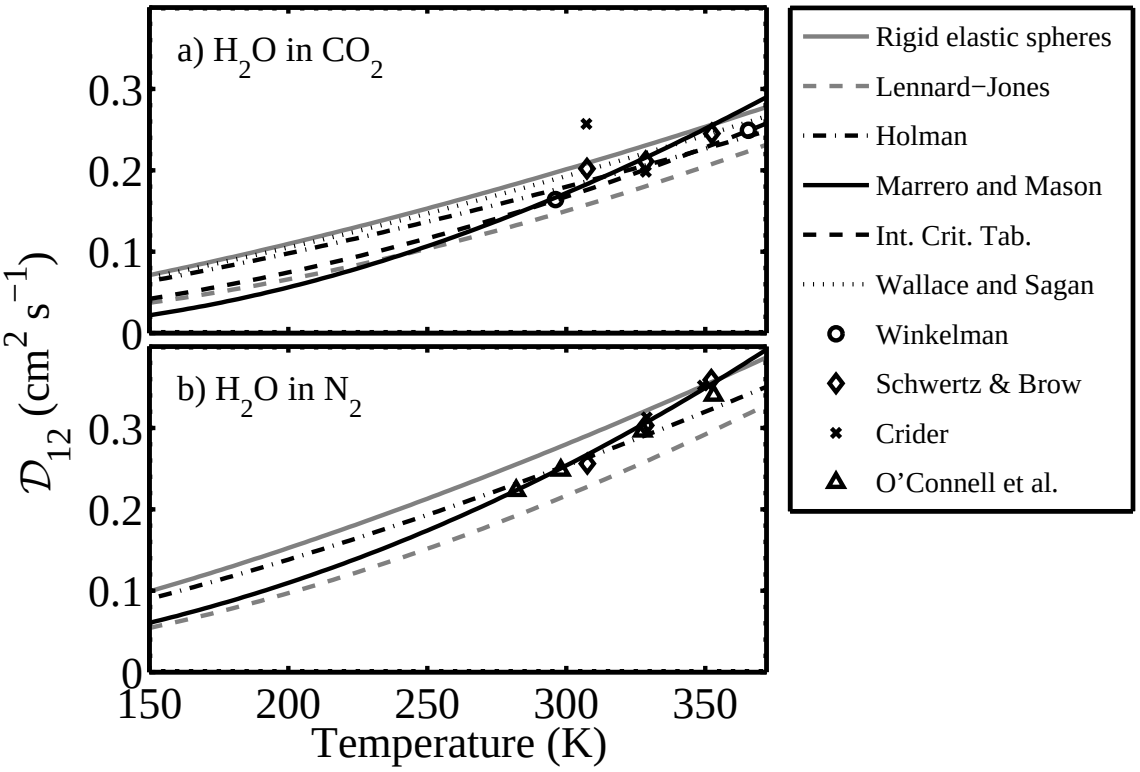

Figure 2.1: Theoretical and measured diffusion coefficients for H_2O in a) CO_2 and b) N_2 as a function of temperature at 1013 mbar. Grey lines are theoretical formulae with model parameters, black lines indicate fits to measured values, and individual markers indicate specific measured values.

The mean free path of H_2O in a dry N_2 atmosphere is longer than in a dry CO_2 atmosphere at the same pressure and temperature by a factor of 1.2.

In a porous solid with interconnected pathways, a gas molecule may collide with another molecule or with the pore walls. When the gas pressure is high, molecule-molecule collisions dominate and the system is said to be in the normal or Fickian regime.

At low pressure, collisions are dominantly between molecules and the walls, and the free path is restricted by the geometry of the void space. In this regime, termed Knudsen diffusion, the presence of other gases no longer affects the transport, and the flux depends only on the density gradient of the species of interest (water in this study) and can be written as (*Mason and Malinauskas*, 1983)

$$J_1 = -D_K \frac{\partial \rho_1}{\partial z}. \tag{2.9}$$

As for Fickian diffusion, the Knudsen diffusion coefficient D_K is proportional to the mean velocity. For example, in a long, straight, circular capillary of radius $r \ll \lambda_1$, the diffusion coefficient at low

pressure is

$$D_{\mathrm{K}} = (2/3)\bar{\nu}_1 r, \tag{2.10}$$

where the mean velocity is $\bar{\nu}_1 = \sqrt{8k_B T/\pi m_1}$ (*Mason and Malinauskas*, 1983; *Clifford and Hillel*, 1986).

Evans et al. (1961) give an expression for D_{K} in materials with interconnected, convoluted pore spaces

$$D_{\mathrm{K}} = \frac{4}{3}\bar{\nu}_1 K_0, \tag{2.11}$$

where K_0 is a structural parameter (with dimensions of length) accounting for both pore geometry and the scattering of the diffusing molecules off the pore walls. They give an expression for K_0

$$\frac{1}{K_0} = \frac{128}{9} n_d \frac{\tau}{\phi} r^2 \left(1 + \frac{1}{8}\pi a_1\right), \tag{2.12}$$

where n_d is the number density of "dust" particles (meaning the porous medium). Here, r is the particle size in the dusty gas model (which may be an average of a particle size distribution), and a_1 is the fraction of molecules that are both scattered diffusely and have their speeds thermalized to a Maxwellian distribution. *Evans et al.* (1961) suggest that a_1 is 1 for most gases. In the case of spherical particles with an average radius $\bar{r}$, n_d can be estimated as $(3/4)(1-\phi)/\pi\bar{r}^3$, giving

$$D_{\mathrm{K}} = \frac{\pi}{8+\pi}\frac{\phi}{1-\phi}\frac{\bar{\nu}_1 \bar{r}}{\tau}. \tag{2.13}$$

These expressions show that D_K is independent of pressure and changes as $T^{1/2}$ with temperature.

Experiments by *Sizemore and Mellon* (2007) have shown that the pore size distributions in disaggregated particles of small size, even pure dust of micron-scale dimensions, tend toward rather large pores, up to 100 microns in diameter or more. Work by Clifford and Hillel has shown that the overwhelming majority of flux in such bimodal or skewed distributions is carried through the largest pores (*Clifford and Hillel*, 1983). Thus, even though a porous regolith may contain particles on the order of 1 micron, the larger size of pores may put diffusion at $p_0 = 6$ mbar largely in the Fickian diffusion regime, with only a minor Knudsen contribution.

At intermediate pressures, collisions with pore walls and with other molecules occur with significant frequency. This "transition region" is defined by the ratio of pore size to mean free path r/λ_1. In the Knudsen regime r/λ_1 is much smaller than 1 and in the Fickian regime r/λ_1 is much greater than 1. Equations (2.2) and (2.9) can be combined by summing their contributions to $\partial\rho_1/\partial z$. Neglecting advection in (2.2) we obtain

$$\frac{\partial \rho_1}{\partial z} = -J_1 \left(\frac{1}{\mathcal{D}_{12}} + \frac{1}{D_K}\right). \tag{2.14}$$

Thus the combined or effective diffusion coefficient may be written

$$D^{-1} = \mathcal{D}_{12}^{-1} + D_{\mathrm{K}}^{-1}. \tag{2.15}$$

This is known as the Bosanquet relation and was discussed by *Pollard and Present* (1948) and more recently described in *Mason and Malinauskas* (1983) in the context of gas diffusion through porous media.

2.5 Tortuosity

Porosity quantifies the reduction in cross-sectional area available for gaseous transport, while tortuosity, τ, is a quantity which characterizes the convoluted nature of the porous pathways followed by diffusing species. The theoretical determination of tortuosity is model dependent and extremely cumbersome for all but the most simple geometries. It is most often the case that the other parameters in equation (2.3), D_{F}, ϕ, and $\mathcal{D}_{12}$, are determined from experiment and τ is calculated from these.

In Chapter 3, experiments are performed at a range of pressures to extract independent Knudsen and Fickian diffusion coefficients. Having thus obtained the purely Fickian diffusion coefficient, equation (2.3) is used with the Fickian diffusion coefficient to determine τ. For the experiments in Chapter 4, variable pressure measurements are not performed. Instead, the method of *Zalc et al.* (2004) is employed, wherein a strictly geometric tortuosity factor, independent of diffusion regime, is derived. Knowledge of the pore space geometries obtained from mercury porosimetry measurements are used to calculate a Knudsen diffusion coefficient. Employing the Bosanquet relation (equation 2.15), D_K and $\mathcal{D}_{12}$ are used with measured values for the effective diffusion coefficient, D, to compute the obstruction factor, and from this determine τ as per equation (2.3).

The free gas diffusivity for either the method employing variable pressures or that using pore geometries may be calculated using one of the formulas in Section 2.3. The experimental procedures described below do not measure $\mathcal{D}_{12}$, and no such measurement of water in CO_2 at Mars surface conditions yet exists in the literature. Care must be taken when using extrapolated values of free-gas diffusivity since there is considerable variation among the expressions available, limiting the accuracy of any calculation involving $\mathcal{D}_{12}$. In the analyses of Chapter 3 and Chapter 4, the extrapolation method of *Wallace and Sagan* (1979) is used to maintain consistency with previous investigators of diffusion on Mars. With different methods, the value of $\mathcal{D}_{12}$ at 250 K and 600 Pa varies between 17.5 and 32.0 $\mathrm{cm^2 s^{-1}}$.

Computation of the Knudsen diffusion coefficient, required for the method described in *Zalc et al.*

(2004), is still more cumbersome. In that work, D_K is written as

$$D_K = \frac{1}{3}\langle l_p \rangle \langle \nu \rangle \left[\frac{\langle l_p^2 \rangle}{2\langle l_p \rangle^2} - \beta \right], \tag{2.16}$$

where ν is the mean molecular velocity ($\nu = \sqrt{8k_BT/\pi m_1}$), $\langle l_p \rangle$ is the first moment of the chord length distribution (*Levitz*, 1993), and β is a series sum of cosine angles between sequential trajectory segments separated by wall collisions. The term outside brackets is the same, within a factor of two, of the simple kinetic expression for the Knudsen diffusion coefficient in straight capillaries defined in equation (2.10). The term in brackets takes into account deviations from exponential path length distributions and Knudsen cosine-law scattering from pore walls, as opposed to random scattering which occurs among gas molecules. Note that in both equations, D_{K} is independent of pressure.

Chords are defined as successive ballistic molecular paths with both ends terminated by a pore wall; they may therefore be smaller or larger than any individual pore. In *Zalc et al.* (2004), the model pore structures used result in nearly exponential chord distributions such that the first term in brackets is near unity. But many real soils may have different distributions and this quantity can vary significantly. *Gille et al.* (2002, 2001) describe a method for determining $\langle l_p \rangle$ from pore diameter distributions determined from mercury porosimetry. The β term, however, depends only on the model selected to describe molecular collisions with pore walls (*Levitz*, 1993). For the frequently used Knudsen cosine law, this gives $\beta = 4/13 = 0.3077$, for porosities up 42% (*Zalc et al.*, 2004) and greater (E. Iglesia, personal communication, 2008), a porosity range which covers all simulants considered in this study except the salt crusts.

The bulk porosity for porous media in these laboratory analyses is determined through a gravimetric method detailed in Section 3.3, and the porosities for various simulants are summarized in Table 3.1. Quantitative measurements of the pore size distribution were made for selected simulant materials at a commercial analytical facility; the analysis results are given in Section 4.3.2.

2.6 Effects Other than Concentration Diffusion

2.6.1 Advection

Mass transfer of a gas results not only from diffusion, which describes the relative motion of gases, but also from advection, where a difference in pressure causes bulk motion of the gas.

The vertical velocity of gas w is given by Darcy's law,

$$w = -\frac{\kappa}{\mu}\frac{\partial p_0}{\partial z}, \tag{2.17}$$

where κ is the intrinsic permeability of the porous medium and μ the dynamic viscosity of the gas.

The total mass flux is the sum of diffusive and advective transport,

$$J_1 = J_{\rm Diff} + J_{\rm Adv} = J_{\rm Diff} + w\rho_1, \tag{2.18}$$

where $J_{\rm Adv} = w\rho_1$.

Most of our experiments take place at a total chamber pressure of ∼600 Pa. At the ice surface, there is a pressure contribution both from the CO_2 in the chamber and the saturation pressure of H_2O. Assuming the pressure difference across the sample equals the saturation vapor pressure, we can set a lower bound on permeability. From equations (2.17), (2.18), and (2.22),

$$J_1 \Delta z = -\rho_0 \frac{\kappa}{\mu} \Delta p_0. \tag{2.19}$$

The viscosity of CO_2 and N_2 at 200 K and 1 bar pressure are 1.00×10^{-5} Pa s and 1.29×10^{-5} Pa s, respectively (*Lide*, 2003). Using measured values of $J_1 \approx 10^{-5}$ kg m^{-2} s^{-1}, $\Delta z = 0.05$ m, and $\rho_0 \approx 0.01$ kg m^{-3} from one of our experiments on 50–80 μm glass beads, the minimum permeability is $\kappa = 3 \times 10^{-12}$ m^2 or 3 darcy. This is similar to permeability values measured for grains tens of microns in size, where $\kappa \sim 10^{-12}$ m^2 (*Freeze and Cheng*, 1979; *deWiest*, 1969).

For sublimation from an impermeable ice layer, the lower boundary condition is $J_2 = 0$. The total mass flux, however, is not zero because the ice is a source of vapor, $J_1 \neq 0$. Mass conservation for species 1 and 2 requires (*Landau and Lifshitz*, 1987)

$$J_1 = -\mathcal{D}_{12}\rho_0 \frac{\partial}{\partial z}\frac{\rho_1}{\rho_0} + w\rho_1 \tag{2.20}$$

$$J_2 = -\mathcal{D}_{12}\rho_0 \frac{\partial}{\partial z}\frac{\rho_2}{\rho_0} + w\rho_2 = 0. \tag{2.21}$$

The ratio of advective to diffusive flux can be obtained by dividing the second term of the first equation by the first term. Solving the second equation for w and substituting, we obtain

$$\frac{J_{\rm Adv}}{J_{\rm Diff}} = \frac{c(z)}{1 - c(z)}. \tag{2.22}$$

The mass concentration of H_2O is denoted by $c = \rho_1/\rho_0$. The total flux is given by

$$J_1 = -\mathcal{D}_{12}\rho_0 \frac{1}{1-c}\frac{\partial c}{\partial z}. \tag{2.23}$$

When the CO_2 column is at rest and H_2O vapor moves outward, the gas mixture as a whole effectively moves outward, and there must always be a pressure difference Δp_0 across the sample that drives this advective flow. On the other hand, the pressure difference can never exceed the saturation vapor pressure over ice. The factor of $1/(1-c)$ is an approximate estimate of the error

due to advective flux being counted as diffusive.

The saturated vapor pressure over ice at 260 K is 195.8 Pa. In 600 Pa of CO_2, this gives a large advective correction factor, $1/(1-c)$, of 1.32. However, at the upper sample surface the partial pressure of water is significantly lower and the correction factor here is found to be 1.01–1.07 in our experiments. The error thus introduced by the average value of c is on the order of 10%. It will be shown that this error is of the same order as the systematic scatter in our experimental determinations of D.

For small c, the advective contribution disappears, $J_1 = J_{\mathrm{Diff}}$, and the pressure difference also becomes negligible. The concentration of water vapor is limited when saturation vapor pressures are low. A practical compromise is reached for experiments between low temperature conditions with small advection contributions and higher temperature conditions which allow faster experimental runs.

On Mars, pressure differences, and therefore advection, can result from winds or thermal expansion. A temperature increase by 30% leads to a thermal expansion by 30% over a thermal skin depth, which is on the order of 1 m for the annual cycle and 3 cm for the diurnal cycle. The expansion thus corresponds to an airflow of 30 cm per year for the annual cycle and 1 cm per sol diurnally. The velocity of water vapor due to concentration differences is estimated as the diffusion coefficient divided by depth such that for $D = 10$ cm^2 s^{-1} and a burial depth of 100 cm, the diffusive flux is 0.01 cm s^{-1} or 9 m per sol, many orders of magnitude faster than thermal expansion.

2.6.2 Thermodiffusion

In a system without concentration gradients, vapor still diffuses due to differences in temperature (*Grew and Ibbs*, 1952). This is known as "thermal diffusion" or "thermodiffusion". The inverse effect, where the diffusion of one gas in another results in the establishment of a transient temperature gradient is known as the "diffusion thermoeffect". The liquid analog to gaseous thermodiffusion is known as the "Soret effect" (*Grew and Ibbs*, 1952). *Chapman and Cowling* (1970) provide a first-order expression for the thermodiffusion ratio $k_T = \mathcal{D}_{\mathrm{T}}/\mathcal{D}_{12}$:

$$k_T = \frac{\mathcal{D}_T}{\mathcal{D}_{12}} = 5(C-1)\frac{s_1\frac{n_1}{n_1+n_2} - s_2\frac{n_2}{n_1+n_2}}{Q_1\frac{n_1}{n_2} + Q_2\frac{n_2}{n_1} + Q_{12}}, \tag{2.24}$$

where

$$\begin{aligned} s_1 &= m_1^2 E_1 - 3m_2(m_2-m_1) + 4m_1m_2A \\ Q_1 &= \frac{m_1}{m_1+m_2}E_1\left[6m_2^2 + (5-4B)m_1^2 + 8m_1m_2A\right] \\ Q_{12} &= 3(m_1^2-m_2^2) + 4m_1m_2A(11-4B) + 2m_1m_2E_1E_2. \end{aligned}$$

Analogous expressions hold for s_2 and Q_2, with interchanged indices. The thermodiffusion coefficient can be positive or negative and vanishes for low concentrations. The parameters A, B, C, E_1, and E_2 depend on the intermolecular forces. For a model of rigid elastic spherical molecules, $A = 2/5$, $B = 3/5$, $C = 6/5$, and $E_1 = (2/5m_1)\sqrt{2/m_2}(m_1 + m_2)^{3/2}\sigma_{11}^2/\sigma_{12}^2$. In the elastic hard sphere model, k_T is independent of temperature and pressure, but it does depend on the proportions of the mixture n_1/n_2 (*Chapman and Cowling*, 1970).

It is conventional to introduce the thermal diffusion factor $\alpha_T = k_T n_0^2/(n_1 n_2)$, which no longer vanishes for low concentrations. Using the formulae above, this factor is at most $\alpha_T \approx 0.8$ for H_2O–CO_2. For H_2O–N_2, the maximum α_T is less than 0.4. The theoretical value of the thermodiffusion ratio is thought to be larger for elastic spheres than for other models of intermolecular forces (*Chapman and Cowling*, 1970). From equation (2.1), we see that thermodiffusion is reduced relative to concentration diffusion by a factor $k_T(\Delta T/T)/\Delta(\rho_1/\rho_0)$. Assuming $n_1 \ll n_2$ and $\Delta n_2/n_2 \ll \Delta n_1/n_1$, this factor is approximately $\alpha_T(m_2/m_1)(\Delta T/T)p_1/\Delta p_1$.

For a typical experiment involving ice loss (Chapters 3 and 4) $\Delta T/T \lesssim 0.01$ and $\Delta p_1/p_1 \approx 0.5$, and thermodiffusion is smaller than concentration diffusion by a factor of $0.4 \times 0.01 \times 0.5 \times 44/18 = 0.005$ or less and is therefore negligible. On Mars, a diurnal temperature amplitude of 30 K around a mean temperature of 210 K has $\Delta T/T \sim 0.14$. It is conceivable that thermodiffusion contributes noticeably to vapor transport on Mars, but concentration diffusion still dominates.

2.6.3 Barodiffusion

"Pressure diffusion" or "barodiffusion" is the relative diffusion of molecular species due to gradients in total pressure. *Landau and Lifshitz* (1987) and *Cunningham and Williams* (1980) provide an expression for the barodiffusion coefficient in a mixture of two ideal gases:

$$k_p = \frac{\mathcal{D}_p}{\mathcal{D}_{12}} = (m_2 - m_1)c(1-c)\left(\frac{1-c}{m_2} + \frac{c}{m_1}\right). \tag{2.25}$$

In a single fluid there is no barodiffusion phenomenon and the coefficient vanishes. For a mixture, the coefficient can be positive or negative, though heavier molecules tend to go to regions of higher pressure. According to equation (2.1), barodiffusion is smaller than concentration diffusion by a factor of $k_p(\Delta p_0/p_0)/\Delta c$. If we assume that $\Delta c \approx c \ll 1$ and use equation (2.25), this factor is about $0.4\Delta p_0/p_0$ in an N_2 atmosphere and $0.6\Delta p_0/p_0$ in a CO_2 atmosphere. Barodiffusion is negligible when $\Delta p_0/p_0 \ll 1$.

Sublimative ice loss experiments in Chapters 3 and 4 take place at a total chamber pressure of ∼600 Pa. At the ice surface, there is a pressure contribution both from the CO_2 in the chamber and the saturation pressure of H_2O, which is at most ∼200 Pa at 260 K. Assuming the pressure difference across the sample equals the saturation vapor pressure, $p_0 = 800$ Pa. This overly pessimistic pressure

difference leads to a barodiffusion contribution of less than 15% of the size of the concentration diffusion.

None of the coefficients $\mathcal{D}_{12}$, $\mathcal{D}_T$, or $\mathcal{D}_p$ depend on gravity, nor does the advective contribution. The potential energy $m_1 g \Delta z$ required to move molecules through the diffusive barrier, or through meters of regolith, is negligible compared with their kinetic energy $(3/2)k_B T$.

Adsorption can significantly effect the transport of water in a non-steady-state environment by attenuating local vapor density gradients and acting as either a source or a sink for water vapor. Adsorption effects will be further discussed in Section 3.6.1 where it will be shown that they are not important on the time scales considered.

2.7 Diffusive Ice Growth

Conservation of mass leads to an expression for the accumulation of ice in pore spaces as a function of time:

$$\frac{\partial \sigma}{\partial t} = -\frac{\partial J_1}{\partial z} = \frac{\partial}{\partial z}\left(D \frac{\partial \rho_1}{\partial z}\right), \tag{2.26}$$

where σ is the density of ice relative to total volume. Hence, ice accumulates in a permeable medium as a humidity gradient supplies water molecules. The presence of ice changes the thermal properties of the regolith by increasing the thermal conductivity of an unconsolidated porous medium. But the formation of subsurface ice is also expected to reduce the diffusivity, and hence the rate of infilling, due to constriction of the pore space. As the pore space is reduced, a regolith with an initially large pore diameter will transition from Fickian diffusion, where molecule-molecule collisions dominate, to Knudsen diffusion wherein most collisions are between molecules and the pore walls. It has been suggested (*Mellon and Jakosky*, 1995) that ice deposited from the vapor phase may completely choke off vapor transport paths. Since subsurface ice has been shown to grow most rapidly near its equilibrium depth (*Mellon and Jakosky*, 1995; *Schorghofer and Aharonson*, 2005), choking would occur first at this level and inhibit diffusion to greater depths. Further discussion of the constriction phenomenon is found in Chapter 5.